

DETERMINATION OF THE STATIC QUADRUPOLE MOMENTS OF THE FIRST 2^+ STATES OF ^{194}Pt , ^{196}Pt , AND ^{198}Pt

J. E. Glenn and J. X. Saladin

University of Pittsburgh, Pittsburgh, Pennsylvania

(Received 11 April 1968)

Static and dynamic electric quadrupole moments of the first 2^+ states in ^{194}Pt , ^{196}Pt , and ^{198}Pt have been determined from Coulomb-excitation cross sections for the scattering of 42-MeV ^{16}O ions measured as a function of scattering angle. The results are compared with recent calculations performed by Kumar and Baranger.

In recent years, interest in the collective behavior of nuclei has been greatly stimulated by the discovery of the large quadrupole moments of the first 2^+ excited states of nuclei which were believed to be spherical.^{1,2} It seemed therefore of particular interest to investigate these moments for nuclei in the transition region around $A \sim 190$ between deformed and "spherical" nuclei. Recently Kumar and Baranger calculated the properties of the low-lying states of even-even nuclei in that region.³ The starting point of these calculations is Bohr's collective Hamiltonian. The seven functions entering Bohr's Hamiltonian, i.e., the potential energy, the three moments of inertia, and the three vibrational inertial parameters, are obtained from a microscopic calculation based upon the pairing-plus-quadrupole model. The Hamiltonian is then diagonalized by an exact numerical method without making any assumptions about the separation of rotation, β motion, and γ motion. The interesting result of their calculation is the prediction of large quadrupole moments Q_{2+} of the first 2^+ states of most nuclei in this region (see Fig. 1). Further, it is predicted that the sign of Q_{2+} changes as one moves from the osmium isotopes to the platinum isotopes.

The present experiment was performed in order to investigate some of these predictions. The determination of the static quadrupole moments is based on higher order effects in Coulomb excitation.⁴ The experimental method used is identical to the one described by us earlier.⁵ 42-MeV O^{16} ions were scattered from thin (5-10 $\mu\text{g}/\text{cm}^2$) isotopically enriched platinum targets (on 10- $\mu\text{g}/\text{cm}^2$ carbon backings). The scattered ions were energy analyzed by an Enge split-pole spectrograph and detected by means of three position-sensitive solid-state detectors. The quantity measured is the ratio $R_{\text{expt}} = d\sigma_{\text{inel}}(2^+)/d\sigma_{\text{el}}$ of the inelastic cross section over the elastic cross section as a function of scattering angle.

The extraction of the quadrupole moments from

the experimental data was accomplished by means of the Coulomb-excitation program of Winther and deBoer.⁶ The nuclear states included in the evaluation as well as the electric-quadrupole matrix elements $M_{if} = -\langle I_i || \mathcal{M}(E2) || I_f \rangle$ between them are listed in Table I. These matrix elements are part of the computer input. The matrix elements M_{12} and M_{22} were varied to obtain a least-squares fit to the experimental data. The values of the matrix elements M_{13} , M_{23} , and M_{24} were taken from McGowan and Stelson⁷ except for M_{23} in Pt^{196} which was obtained by assuming the same ratio of M_{23}/M_{12} as in Pt^{194} . The matrix elements M_{33} , M_{44} , and M_{34} were set equal to zero. This is a good approximation since M_{34} is expected to be small and the influence of M_{33} and M_{44} on the population of level 2 is negligible. The quadrupole moment Q_{2+} of

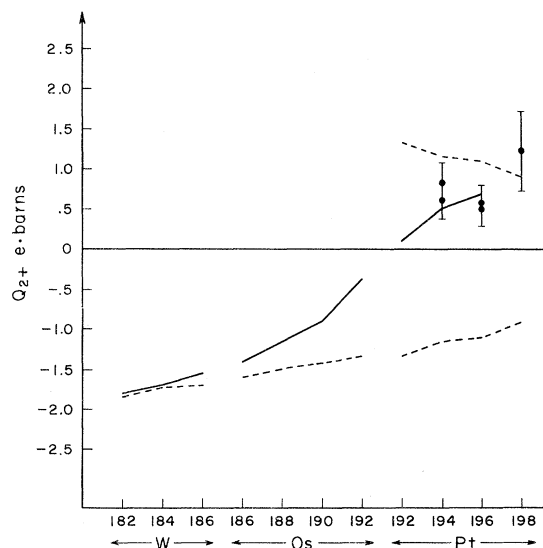


FIG. 1. Experimental values and theoretical predictions of Q_{2+} . The circles represent the measured values. The solid curve connects values predicted by Kumar and Baranger. The dashed curves are calculated from experimental $B(E2)$'s using the rotational-model relationship $(M_{22}/M_{12})^2 = 10/7$. For platinum, both prolate and oblate intrinsic shapes are considered.

Table I. Level information used in computer calculation of the Coulomb-excitation cross sections.

Isotope	Level Index n	Excitation Energy (MeV)	Spin And Parity	M _{1n}	M _{2n}	M _{3n}	M _{4n}
194	1	0.000	0 ⁺	0	M ₂₁	+0.093	0
	2	0.328	2 ⁺	M ₁₂	M ₂₂	±1.07	+2.062
	3	0.622	2 ⁺	+0.093	±1.07	0	0
	4	0.811	4 ⁺	0	+2.062	0	0
196	1	0.000	0 ⁺	0	M ₂₁	+0.036	0
	2	0.356	2 ⁺	M ₁₂	M ₂₂	±1.012	+1.844
	3	0.689	2 ⁺	+0.036	±1.012	0	0
	4	0.877	4 ⁺	0	+1.844	0	0
198	1	0.000	0 ⁺	0	M ₂₁		
	2	0.408	2 ⁺	M ₁₂	M ₂₂		

the first 2⁺ state and the $B(E2)$ for a transition between the ground state and the first 2⁺ state are related to the matrix elements M_{12} and M_{22} through the equations

$$B(E2, 0^+ \rightarrow 2^+) = |M_{12}|^2$$

and

$$Q_{2+} = -0.758 M_{22}.$$

An ambiguity in the evaluation of the data arises due to the fact that the relative phases between the matrix elements M_{13} and M_{23} are not known. The various possibilities are best discussed⁸ in terms of the sign of the product $M_{12} \times M_{23} M_{13} M_{22}$ which is independent of phase convention. The data were analyzed using either sign

Table II. $B(E2)$ and Q_{2+} values from a least-squares analysis.

Isotope	Sign of ($M_{12}M_{23}M_{13}M_{22}$)	$B(E2)$ ($e^2 b^2$)	Q_{2+} ($e b$)
194	+	1.65 ± 0.02	0.62 ± 0.18
194	-	1.65 ± 0.02	0.84 ± 0.16
196	+	1.50 ± 0.03	0.49 ± 0.18
196	-	1.50 ± 0.03	0.56 ± 0.21
198	0	1.01 ± 0.03	1.22 ± 0.50

for this product. The results are listed in Table II are shown in Fig. 1. The theory of Kumar and Baranger predicts the sign of the above product to be negative, which corresponds to the larger Q_{2+} values. Figure 1 also shows the results of the Kumar-Baranger theory and the predictions of the pure-rotator model. The sign of Q_{2+} from the rotator model depends upon whether one assumes the intrinsic shape to be prolate or oblate; both possibilities are shown for the platinum isotopes. The measured quadrupole moments are within experimental uncertainties in agreement with the predictions of the Kumar-Baranger theory. It is of particular interest that the theory predicts the sign of the quadrupole moments in the platinum region correctly. Experiments on the osmium isotopes are in progress in order to investigate the predicted change in sign.

It is a pleasure to acknowledge stimulating discussions and correspondence with Professor A. Winther, Professor M. Baranger, and Professor K. Kumar. We are very much indebted to R. J. Pryor and J. R. Kerns for extensive help in data taking.

*Work supported by the National Science Foundation.

¹J. deBoer, R. G. Stokstad, G. D. Symons, and A. Winther, Phys. Rev. Letters **14**, 564 (1965).

²J. deBoer and J. Eichler, in Advances in Nuclear Physics, edited by M. Baranger and E. Vogt (Plenum Press, Inc., New York, 1968), Vol. 1.

³K. Kumar and M. Baranger, *Phys. Rev. Letters* **17**, 1146 (1966).

⁴For a discussion of the underlying theory see Ref. 2.

⁵J. E. Glenn and J. X. Saladin, *Phys. Rev. Letters*

19, 33 (1967).

⁶Aage Winther and Jorrit deBoer, in Coulomb Excitation, edited by K. Adler and A. Winther (Academic Press, New York, 1966).

⁷F. K. McGowan and P. H. Stelson, *Phys. Rev.* **122**, 1274 (1961), and private communication.

⁸A. Winther, private communication.

EXPERIMENTAL EVIDENCE FOR THE DOUBLE-BETA DECAY OF Te^{130} †

T. Kirsten and O. A. Schaeffer

Department of Earth and Space Sciences, State University of New York, Stony Brook, New York

and

E. Norton and R. W. Stoenner

Department of Chemistry, Brookhaven National Laboratory, Upton, New York

(Received 1 April 1968)

It is shown that double-beta decay occurs in nature. The half life of Te^{130} is $10^{21.34 \pm 0.12}$ yr.

Attempts to detect double-beta decay directly by means of coincidence techniques or nuclear emulsions have not led to an actual observation of double-beta decay.¹ Lower limits for the half lives of different isotopes were established. The most studies were made on Ca^{48} .¹

Another approach is to detect the accumulation of the decay product during geological time periods ($\sim 10^9$ yr) in those minerals which are rich in a suspected $\beta\beta$ -active isotope. Two very suitable cases for this method are the decays of $\text{Te}^{130} \beta\beta \text{Xe}^{130}$ and $\text{Se}^{82} \beta\beta \text{Kr}^{82}$.²

An anomalous isotopic composition of xenon extracted from tellurium minerals has been reported repeatedly.^{3,4} In all cases, surplus amounts of Xe^{129} , Xe^{130} , and Xe^{131} were superimposed on the general pattern of xenon of atmospheric composition. These findings have not been accepted¹ as proof for the double-beta decay of Te^{130} since the Xe^{130} anomaly was always accompanied by Xe^{129} and Xe^{131} excesses not yet completely understood. Rather, it was suspected that all three anomalies might result from the same unknown mechanism. In some cases, the xenon spectrum was even more confused by an additional fission xenon component which complicated the computation of the atmospheric Xe^{130} correction. The Xe^{130} excess was arrived at only by a rather involved calculation which included large uncertainties. The magnitude of the Xe^{130} excess has been less than 6% of the total xenon amount in all samples studied by other authors. In addition, the calculated half lives of Te^{130} were based on assumed geological ages of the miner-

als rather than on age determinations of the tellurium ores themselves.

To prove that Te^{130} is $\beta\beta$ active one has to show that the Xe^{130} excess is unambiguously due to double-beta decay. In addition, a calculated half-life can only be accepted if it is based on radioactive dating of the mineral.

We have analyzed the isotopic composition of xenon extracted from a native tellurium ore from the Good Hope mine (Colorado).⁵ We found a large excess of Xe^{130} not accompanied by any other anomalies.⁶ In uncrushed samples not exposed to air contamination, the excess Xe^{130} amounts to about 70% of the total xenon and the ratio $\text{Xe}_{\text{excess}}^{130}/\text{Xe}_{\text{atmospheric}}^{130}$ is higher than 50. The Xe^{130} excess does not constitute a small anomaly on the border of detectability but determines the pattern of the xenon spectrum (Fig. 1).

The absence of other xenon anomalies rules out processes other than double-beta decay which might possibly result in a Xe^{130} excess.^{7,2} The production of Xe^{130} via two successive single-beta decays is impossible since the mass excess of I^{130} is 477 ± 35 keV larger than the mass excess of Te^{130} .⁸ We must then conclude that the Xe^{130} excess is due to double-beta decay of Te^{130} .

From the amount of $\text{Xe}_{\text{excess}}^{130}$, the tellurium concentration, and the gas-retention age of the mineral, the half-life of Te^{130} can be calculated. We determined the K-Ar age of the ore and obtained an age of 1.31 ± 0.14 Gyr. The age is considered to be reliable since it is consistent with the geological situation of the ore deposit.⁹